Supporting information

A novel albumin nanocomplex containing both small interfering RNA and gold nanorods enables synergetic anticancer therapeutics by employing both thermal ablation and RNA interference

Jin-Ha Choi,[a] Hai-Jin Hwang,[b] Seung Won Shin,[c] Jeong-Woo Choi,[a,b] Soong Ho Um,[*c,d] and Byung-Keun Oh[*a,b]

Characterization of BSA Nanoparticles: To optimize the conditions for particle synthesis, the effect of pH prior to the addition of ethanol was investigated. As shown in Figure S1, an increased pH resulted in a decreased amount of BSA particles with a more negative surface charge. With respect to cellular uptake efficiency and the successful encapsulation of both siRNA and AuNRs, BSA nanoparticle synthesis was found to be optimal at pH 6. The concentration of synthetic particles was measured by manually counting the number of BSA particles using TEM images (Figure S2). To ensure accuracy, five representative images were obtained at three different concentrations (1/5, 1/25, and 1/125 dilutions of the original 20 mg/ml solution). The numbers of synthetic particles were calculated from the ratio of the area of each image to that of the TEM grid.

Determination of the Method for Rod Encapsulation in the BSA complexes: To determine the most efficient synthetic method for rod encapsulation, desolvation was first performed by

simply mixing BSA with functionalized AuNRs (Figure S3a). The AuNRs were sequentially modified with SH-PEG-amine, SPDP, and thiolated siRNA to induce the AuNR-mediated cleavage of siRNA via its disulfide linkage. However, as shown in Figure S3a, this method had serious drawbacks, including the absence of AuNRs in the resultant BSA complexes and the aggregation of AuNRs after successive reactions. The second attempt included two steps. In the first step, the AuNR surface was precoated with siRNA via direct chemical bonding between the Au nanorods and the thiol compound of the siRNA; in the second step, desolvation was performed by mixing the functionalized rods with BSA. This attempt also failed to encapsulate the AuNRs in the BSA complexes, and the AuNRs maintained their original shape (Figure S3b). Finally, the AuNRs were pretreated with SH-BSA and subsequently desolvated using a mixture consisting of BSA-functionalized AuNRs, bare BSA, and siRNA (Figure S3c).

UV/vis Spectra of AuNRs and SREB Complexes: To determine the optical properties of the SREB complexes, the UV/vis spectrum of the complexes was compared with the spectrum of naked BSA particles and the spectrum of AuNRs, which ranged from 450 nm to 800 nm (Figure S4a). The absorption peaks for the AuNRs and the SREB complexes were separated into two regions, near 520 nm and 750 nm. To identify the spectrum of the SREB complexes, the absorption value of the BSA particles was subtracted from the absorption value of the SREB complexes (Figure S4d).

Immobilization of the Targeting Ligand on the SREB Complexes: Anti-ErbB-2 antibodies, which are specific for the target breast cancer cells, were immobilized on the SREB complexes via a streptavidin-biotin interaction. The SREB complexes were first functionalized with amine-PEG-biotin to inhibit self-aggregation and provide a longer circulation time *in vivo*. Next, the functionalized SREB complexes were incubated with

streptavidin-labeled anti-ErbB-2 antibodies. As shown in Table S1, the binding efficiency of the streptavidin-labeled antibodies to the nanocomplexes was five-fold greater than the binding efficiency achieved through physical adsorption. Binding efficiencies were determined by quantifying the amount of unbound antibodies using the Bradford method.

Cytotoxicity Test: The cytotoxicity of the therapeutic nanocomplexes was measured using the MTT assay. Treatment of SK-BR-3 cells with either BSA nanoparticles or SREB complexes, at concentrations ranging from 5 pM to 40 pM and an incubation length of 24 h, did not significantly affect viability. In contrast, the AuNRs were severely cytotoxic. This finding was likely due to residual CTAB components in the solution (Figure S5).

Enzymatic Degradation of SREB Complexes: For SREB complex-mediated delivery of siRNA, BSA degradation is critical. This degradation can occur either enzymatically via intracellular proteases or thermally via NIR irradiation. To analyze the mechanism by which the SREB complexes are degraded, we investigated the effects of 5 μg/ml trypsin treatment and thermal treatment on the complexes. As shown in Figure S6, degraded BSA and encapsulated rods were observed after enzymatic treatment. However, AuNR-generated heat did not affect the decomposition of SREB complexes (Figure S7). Interestingly, the mean diameter of the particle complexes tended to increase at higher temperatures upon photothermal treatment.

Kinetics of siRNA Release from the SREB Complexes*:* To determine the kinetics of siRNA release, the SREB complexes were treated with trypsin for 48 h to induce degradation of BSA. As shown in Figure S8, encapsulated siRNA was continuously released from the SREB complexes for 48 h in the presence of trypsin. Moreover, siRNA release did not occur in the absence of trypsin. Therefore, the SREB complexes enabled the sustained release of siRNA for a consistently strong RNA*i*-induced apoptotic effect.

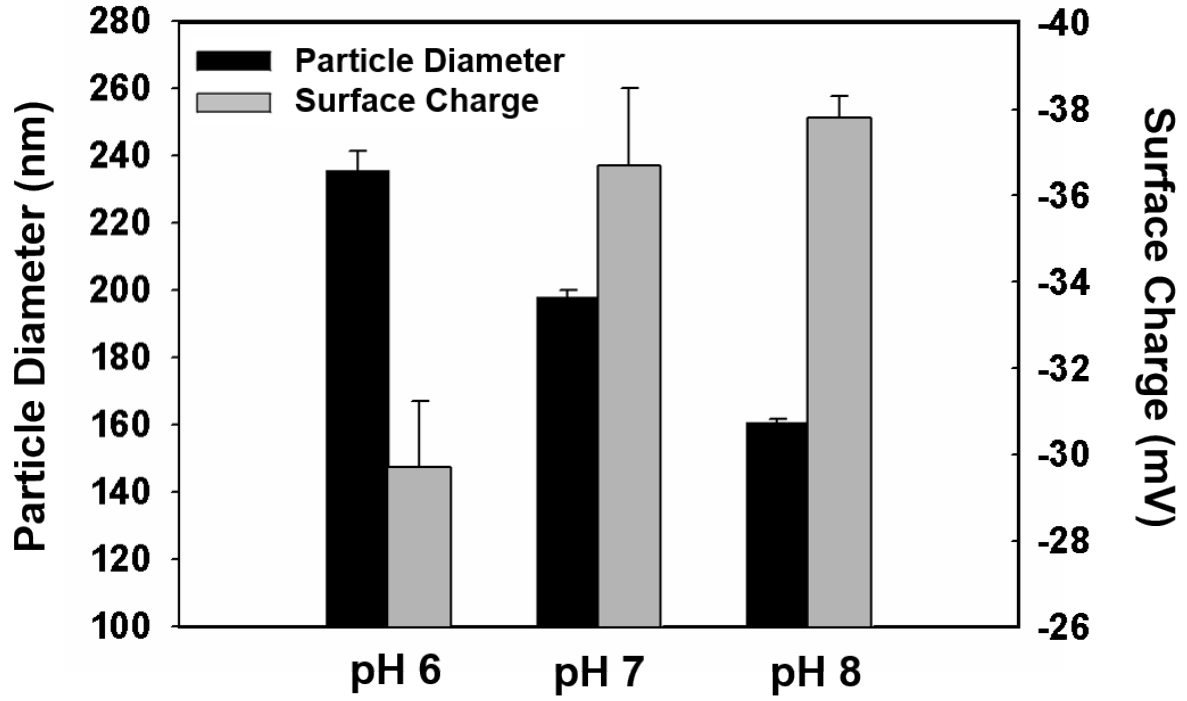

Figure S1. Characterization of the relationship between particle diameter and surface charge of the BSA nanoparticles with respect to pH. Black bars, diameters of the particles used; gray bars, negative surface charges. Data were expressed as mean ± S.E.M. (n = 4).

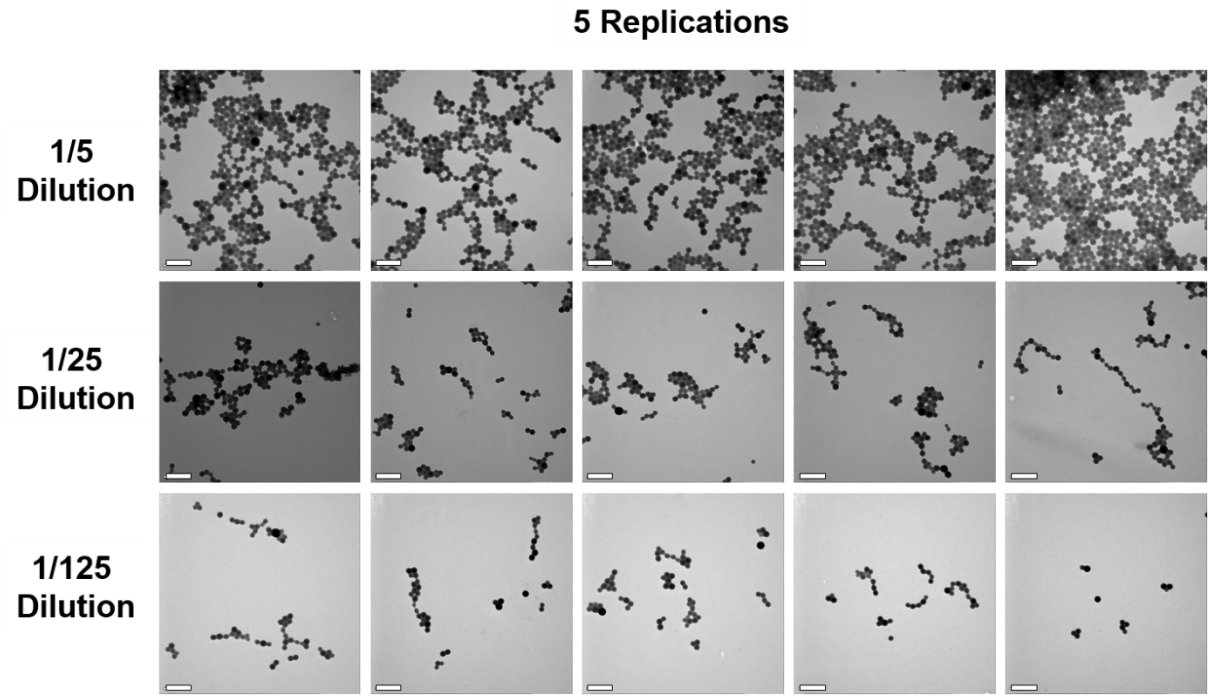

Figure S2. TEM images of BSA nanoparticles at three different dilutions. The stock solution contained 20 mg/ml BSA. The first, second, and third rows show BSA nanoparticles that were diluted five-fold, 25-fold, and 125-fold, respectively. Scale bars, 1 μm. Each image is representative of five different replicates.

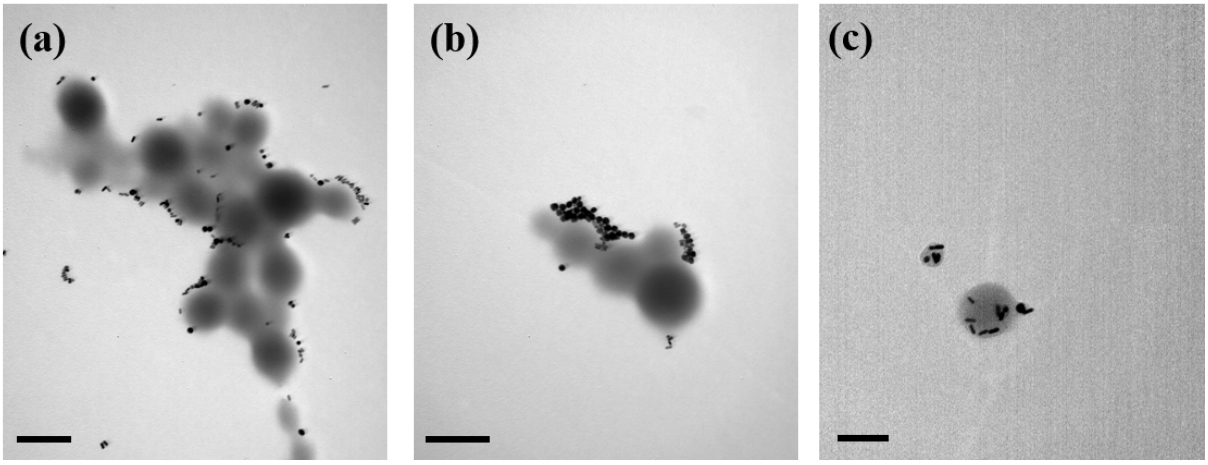

Figure S3. TEM images of siRNA- and gold nanorod (AuNR)-encapsulated BSA complexes (SREBs) manufactured by a variety of preparative methods. (a) Pretreatment of siRNA on the surfaces of the AuNRs using simple sequential conjugate chemistry. SH-PEG-NH_2, SPDP, and SH-siRNA were allowed to react, followed by desolvation with a mixture of functionalized rods and BSA. (b) Pretreatment of siRNA on the surface of the AuNRs using direct chemical bonding between the Au nanorods and the thiol compound of the siRNA, followed by desolvation with a mixture of the functionalized rods and BSA. (c) Simultaneous encapsulation of both siRNA and SH-BSA-functionalized rods by BSA. Scale bars, 200 nm.

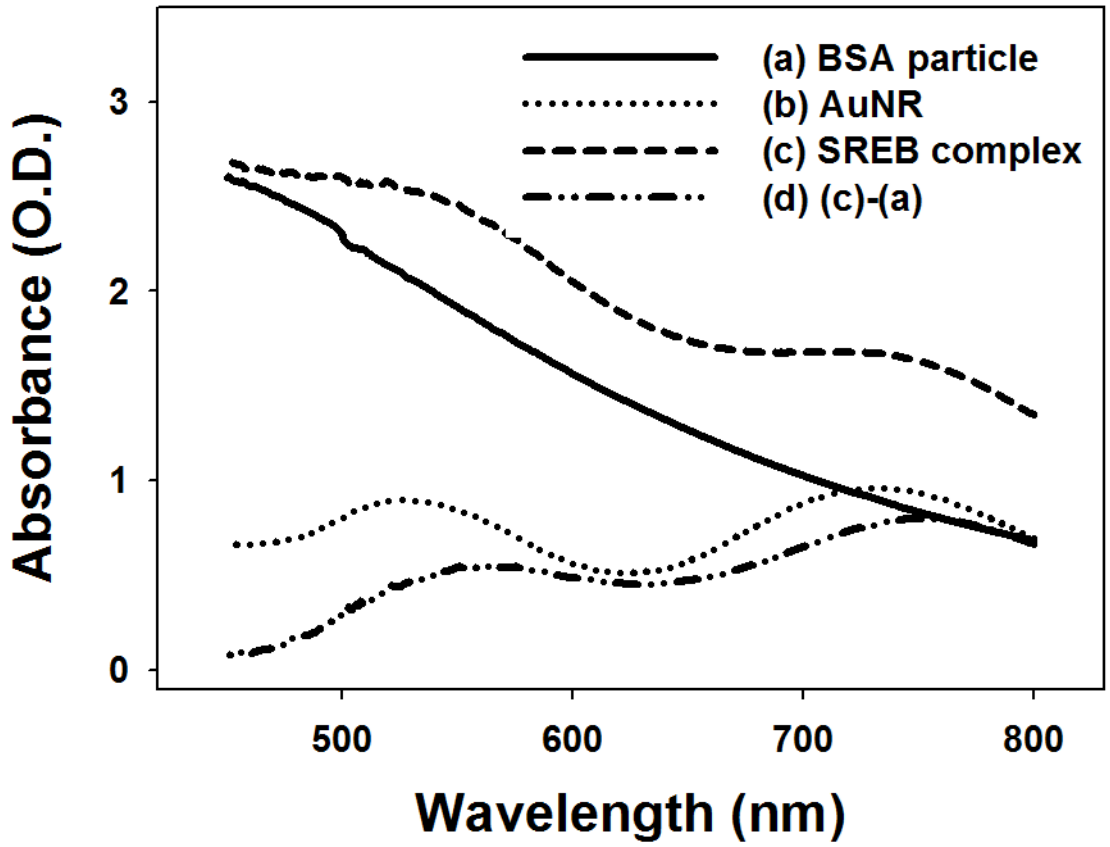

Figure S4. UV/vis absorbance spectra of (a) BSA nanoparticles (straight line), (b) AuNRs (dotted line), (c) SREB nanocomplexes (dashed line). The panel (d) (dotted/dashed lines) indicates the values obtained by subtracting (a) from (c).

	Supernatant Abs.	Supernatant Conc.(μg/ml)	Attached Conc.(μg/ml)
SREB + Ab (Physical adsorption)	0.22	18.34	1.66
SREB + Biotinylated Ab (Streptavidin-Biotin)	0.16	11.45	8.55

Table S1. Comparison of the efficiencies of ligand functionalization using physical absorption vs. the biotin-streptavidin interaction immobilization method. Efficiencies were determined by measuring the supernatant concentrations of unbound ligand.

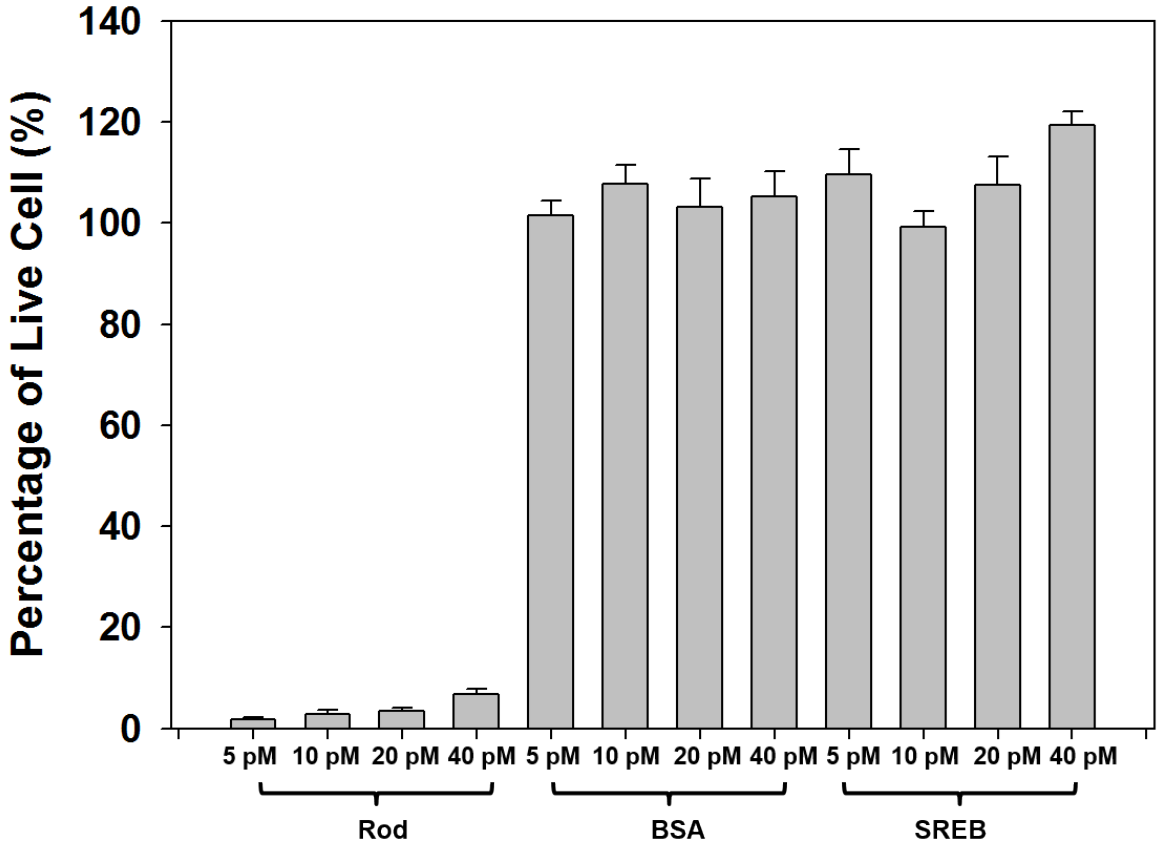

Figure S5. Cytotoxicity of the materials used in the experiments. AuNRs, BSA nanoparticles, and SREB nanocomplexes were tested in the range of 5 pM to 40 pM. Data were expressed as mean ± S.E.M. (n = 4).

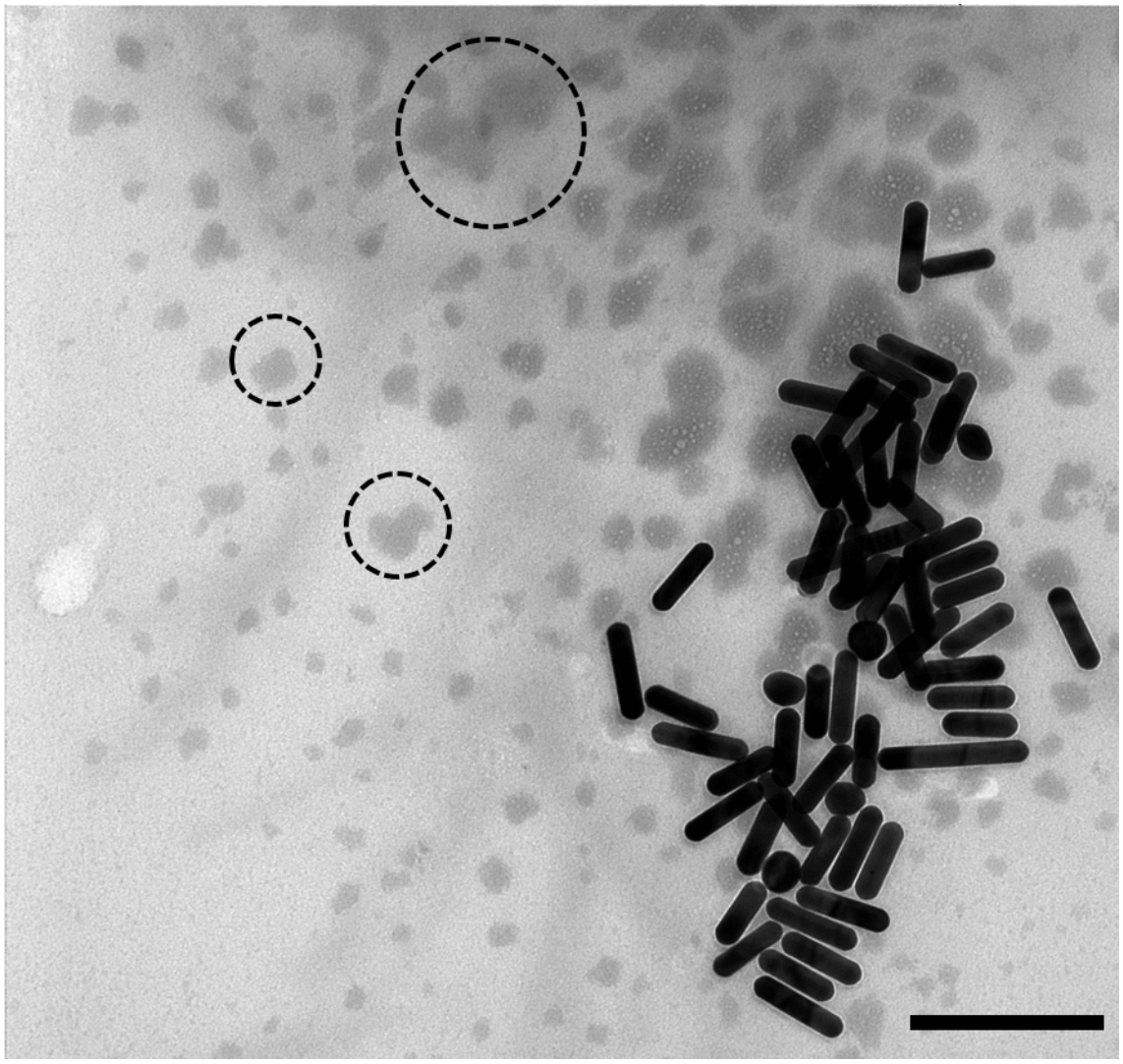

Figure S6. TEM image of proteolytically degraded SREB nanocomplexes. Dark gray dots, remnants of BSA particles; black dots, AuNRs. The scale bar is 200 nm.

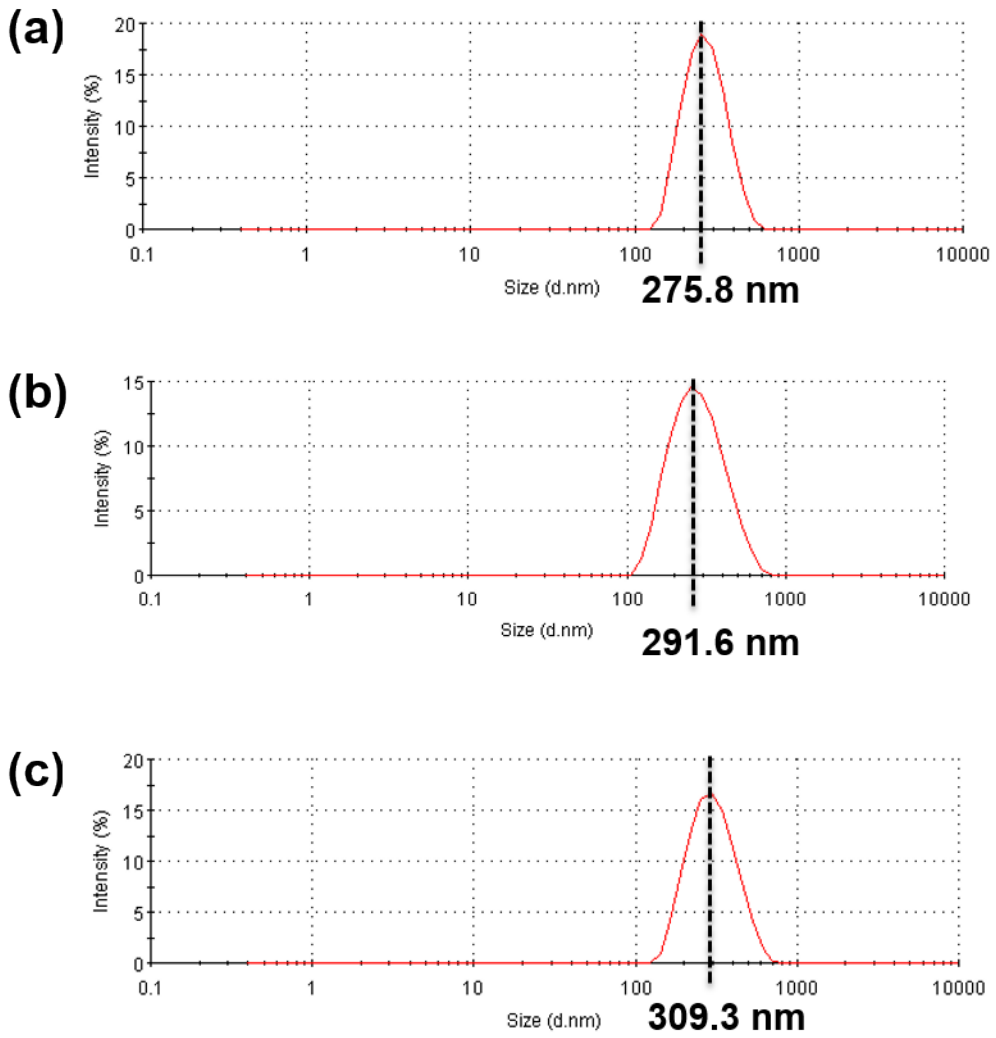

Figure S7. Dynamic light scattering (DLS) of BSA nanoparticles after thermal treatment at (a) 40 °C, (b) 50 °C, and (c) 60 °C for 10 min.

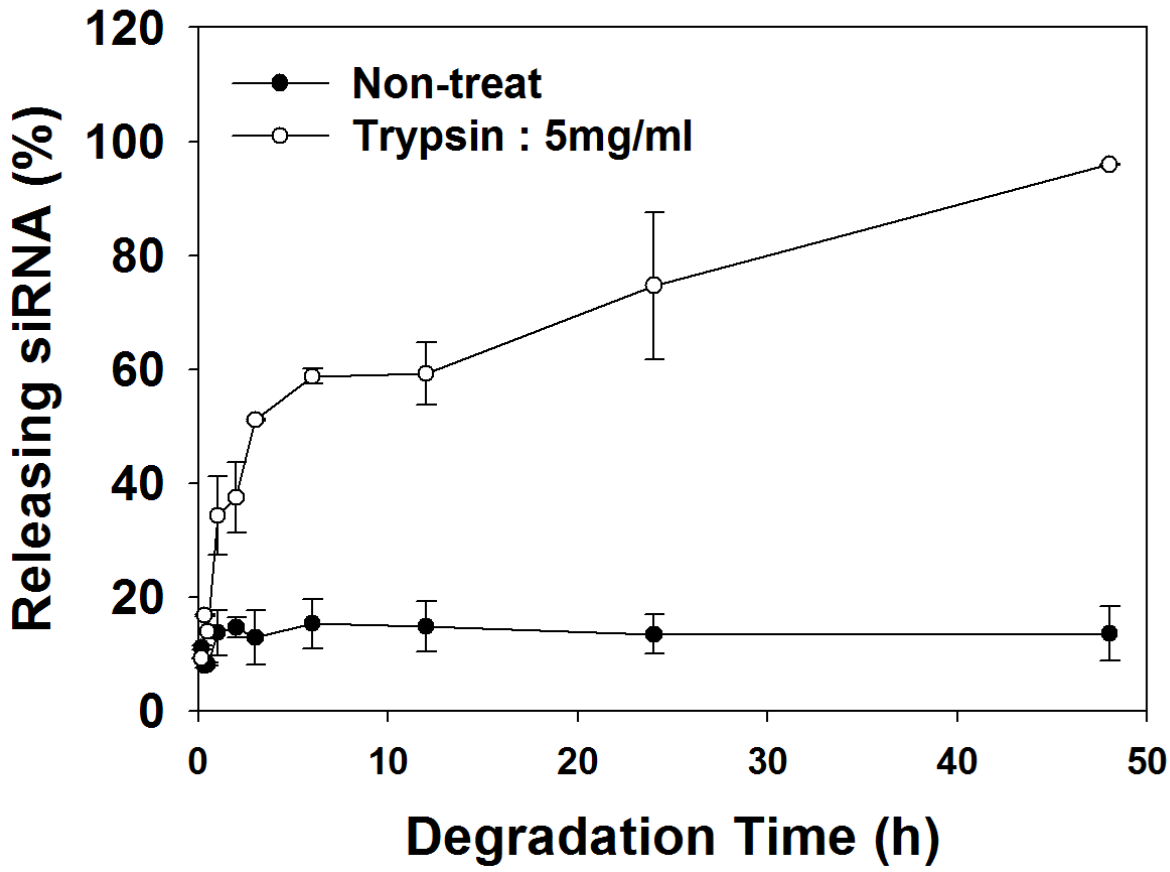

Figure S8. Release kinetics of siRNA drugs from the SREB nanocomplexes. Data were expressed as mean ± S.E.M. (n = 3).